*Ecology Letters*, (2004) **7**: 547–556 doi: 10.1111/j.1461-0248.2004.00612.x

REPORT

# Complex structural effects of two hemispheric climatic oscillators on the regional spatio-temporal expansion of a threatened bird

**Pablo Almaraz[1]* and Juan A. Amat[2]**
*[1]Departamento de Biología Animal y Ecología, Facultad de Ciencias, Universidad de Granada, E-18071 Granada, Spain*
*[2]Estación Biológica de Doñana, Consejo Superior de Investigaciones Científicas, Apartado 1056, E-41080 Sevilla, Spain*
**Correspondence: E-mail: almaraz@fedro.ugr.es*

## Abstract

Links between climatic conditions in the eastern equatorial Pacific and extratropical ecological processes remain unexplored. The analysis of a 20-year time series of spatial and numeric dynamics of a threatened Mediterranean bird suggests, however, that such couplings can be remarkably complex. By providing a new ecological time-series modelling approach, we were able to dissect the joint effects of the El Niño/Southern Oscillation (ENSO), the North Atlantic Oscillation (NAO), regional weather, population density and stochastic variability on the expansion dynamics of the White-headed duck (*Oxyura leococephala*) in Spain. Our results suggest that the spatial and numeric dynamics of ducks between peak brood emergence and wintering were simultaneously affected by different climatic phenomena during different phases of their global cycles, involving time lags in the numeric dynamics. Strikingly, our results point to both the NAO and the ENSO as potentially major factors simultaneously forcing ecological processes in the Northern Hemisphere, and suggest a new pathway for non-additive effects of climate in ecology.

## Keywords

Climate fluctuations, El Niño/Southern Oscillation, mathematical modelling, Mediterranean basin, North Atlantic Oscillation, *Oxyura leucocephala*, population dynamics, statistical modelling, structural equations with latent variables.

*Ecology Letters* (2004) 7: 547–556

## INTRODUCTION

Exploring the interface of climate and ecological systems is a central challenge of current environmental research (Sæther *et al.* 2000; Stenseth *et al.* 2002). The use of proxy indexes of large-scale climatic phenomena, which reduce the complex spatio-temporal variability of weather fluctuations in a single measure, is prompting a growing body of empirical studies on the ecological effects of climate (Stenseth *et al.* 2002, 2003). For instance, the North Atlantic Oscillation (NAO) and the El Niño/Southern Oscillation (ENSO) are currently recognized as main planetary sources of interannual climatic variability (Hurrell 1995; Allan *et al.* 1996; Trenberth *et al.* 1998; Visbeck *et al.* 2001; Stenseth *et al.* 2003) and they are also being increasingly acknowledged as a major source of population variability (Bjørnstad & Grenfell 2001; Ottersen *et al.* 2001; Stenseth *et al.* 2002), which is broadening the everlasting debate of extrinsic vs. intrinsic factors in population regulation (Bjørnstad & Grenfell 2001). Indeed, by using climate indexes, a rich array of complex climatic effects on population dynamics can be documented, including, for instance, interactive (non-additive) effects (Sæther *et al.* 2000; Coulson *et al.* 2001; Chávez *et al.* 2003), regime shifts (Rodó *et al.* 2003; Durant *et al.* 2004) and time lags (Thompson & Ollason 2001; Almaraz & Amat 2004).

Although individuals experience climatic conditions at local and regional scales, these conditions can be highly heterogeneous in space and time (Plisnier *et al.* 2000; Stenseth *et al.* 2002). Additionally, fluctuations of local weather are usually teleconnected with climatic oscillators operating at very large spatial scales (Hurrell 1995; Allan *et al.* 1996; Ottersen *et al.* 2001; Stenseth *et al.* 2003), with centres of action sometimes located at the opposite hemisphere (e.g. Hurrell 1995; Rodó *et al.* 1997; Moron & Ward 1998; van Oldenborgh *et al.* 2000). However, most studies linking ecological processes to the NAO and the ENSO have been conducted in geographical regions close

©2004 Blackwell Publishing Ltd/CNRS

to their centres of action (e.g. Polis *et al.* 1997; Sæther *et al.* 2000; Sillet *et al.* 2000; Holmgren *et al.* 2001; Aanes *et al.* 2002; Lima *et al.* 2002; Lekve *et al.* 2003; Durant *et al.* 2004), so the ecological responses outside these areas are poorly known, for instance, at the population dynamics level (Ramos *et al.* 2002; Ogutu & Owen-Smith 2003). Moreover, the understanding of the mechanistic basis underlying a given ecological response to climate is incomplete without a full characterization of the relationship between large-scale climate and local weather (Stenseth *et al.* 2003), but this 'climatic downscaling' is usually neglected in ecological studies. For instance, Ramos *et al.* (2002) recently found concurrent correlations between the breeding successes of a seabird in the Indian Ocean and both local weather and ENSO indexes; however, their analyses and interpretations were confounded by the teleconnection of both local and large-scale climate.

Here we report for the first time on the simultaneous effects of northern (NAO) and southern (ENSO) hemispheric fluctuations in climate on the spatio-temporal dynamics of a natural population throughout most of its world distribution range. We first propose a substantive hypothesis accounting for non-additive effects of climatic fluctuations on the seasonal spatial and numeric expansion of the globally threatened *Oxyura leucocephala* (the white-headed duck) in the south-western Palaearctic during a 20-year period, and then translate it into a combination of a measurement model and a structural model (Bollen 1989). Recent evidence (Almaraz & Amat 2004) suggests that seasonality is a key process in the spatio-temporal dynamics of *O. leucocephala* in southern Europe; however, although at any one time a positive abundance–area relationship can be found throughout the distribution range of ducks, spatial and numeric recruitment processes taking place between breeding and wintering are largely uncoupled. Therefore, by using a novel approach to implement the neglected climatic downscaling in a single model, our main goal in this paper will be to explore if different large-scale climatic phenomena may be simultaneously forcing spatial and numeric dynamic processes in this species, a question with central implications beyond ecological theory. For example, although the ENSO effects on Palaearctic climate are currently uncertain (IPCC 2001), severe climatic and ecological impacts are forecasted for this region under climate warming scenarios (IPCC 2001; Mooney *et al.* 2001; Christensen & Christensen 2003). Thus, given the current positive phases of both the NAO and the ENSO correlated with global warming (Allan *et al.* 1996; IPCC 2001; Visbeck *et al.* 2001), untangling the links between large-scale climate and ecological processes in the western Palaearctic can yield valuable insights into the behaviour of natural ecosystems under climate change scenarios (Mooney *et al.* 2001).

## MATERIAL AND METHODS

### Location and population data

*Oxyura leucocephala* is a small diving, strongly territorial duck with highly fragmented populations in north-eastern Africa, southern Spain and Central Asia (Green & Hughes 2001). World population was estimated at 14 000–20 000 in the year 2000 (Green & Hughes 2001); nearly the 30% of the world population of the species (4500 birds) gathered in Spain in this year (Green & Hughes 2001; Almaraz & Amat 2004). Population dynamics data used in this study consist of direct counts gathered simultaneously throughout the study area (124 habitat patches in south-western Spain), during January (wintering) and June (peak brood emergence during the breeding season) (see Almaraz & Amat 2004 for further details on sampling methodology).

As the population expanded in an exponential fashion during the study period (Almaraz & Amat 2004) the difference in $\log_e$-range size in wintering ($S_w$) and $\log_e$-range size during breeding ($S_b$) is an estimate of seasonal range dynamics ($\Delta S_b = S_w - S_b$); on the other hand, numeric recruitment of broods during the breeding season ($\Delta N_b$) was calculated as the difference in $\log_e$-population size in wintering ($N_w$) and $\log_e$-population size during breeding ($N_b$). Thus, we will work with full seasonal models (Almaraz & Amat 2004). Brood recruitment is positively correlated to overwintering survival ($r = 0.601$, $n = 20$, $P = 0.004$), so recruitment is also an estimate of interannual numeric expansion. A regional estimate of population density ($D_r$, birds per km$^2$) was used in the analyses as a weighted index of spatial crowding of birds (see Almaraz & Amat 2004 for details). We have used this measure because the study area conforms to a highly dynamic *patchy* population rather than to a network of local, partially isolated populations connected by migration (Almaraz & Amat 2004; see Harrison 1994).

### Climatic data

As regional-scale climatic descriptors, we used records on summer (July to August) and winter (November to December) precipitation from the year 1979 to 2000 throughout the distribution range of the species in the study area (see Almaraz & Amat 2004). Large-scale climatic data comprise the multivariate ENSO index (MEI: http://www.cdc.noaa.gov/~kew/MEI/mei.html; Wolter & Timlin 1993) and the NAO index (http://www.cgd.ucar.edu/~jhurrell/nao.html, Hurrell 1995). The MEI index has been suggested by Wolter & Timlin (1993) as a better descriptor for exploring ENSO teleconnections with extratropical regions. Precipitation values were regressed against NAO and ME monthly index values with lags up to 12 months using a distributed-lags analysis; according to this analysis, summer (June to August) and winter (November to January) values for both proxy

©2004 Blackwell Publishing Ltd/CNRS

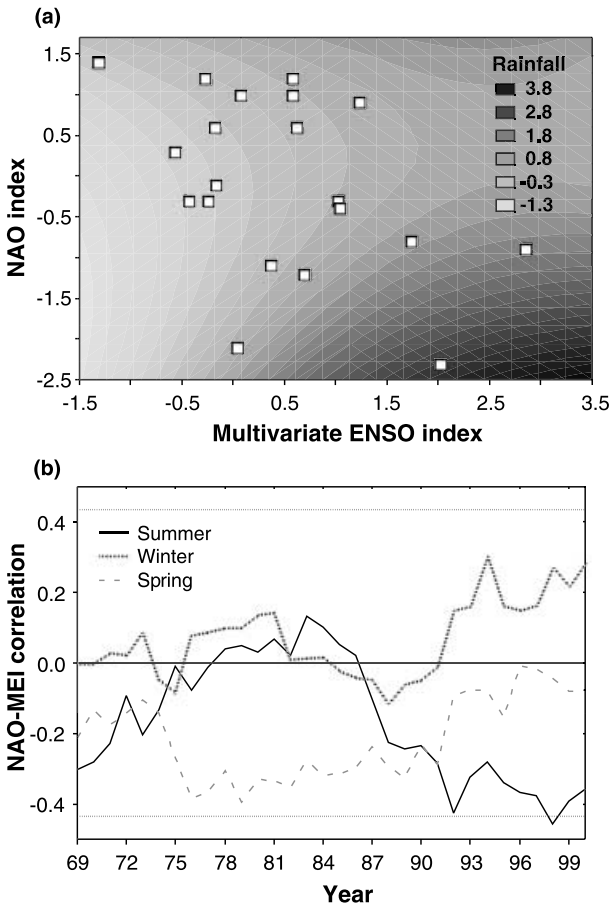


**Figure 1** Climatic data used in the analysis. (a) Response surface depicting the joint effects of the multivariate ENSO index and the NAO index on standardized regional rainfall variability, during the boreal summers of the period 1980–2000 (see text); only for illustrative purposes, the surface was fitted using a bicubic spline smoothing algorithm. (b) 20 years running Pearson's correlation coefficient (sliding windows; see, e.g. Rodó *et al.* 2003) between the NAO and the ENSO during the boreal summer, winter and spring seasons from 1950 to 2000. Horizontal dotted lines in the graph indicate statistical significance of individual correlations at a nominal 0.05 level.

indexes yielded the largest partial regression coefficients for the summer and winter precipitation subsets, respectively, so those values were used in the analysis (see Fig. 1a).

## STRUCTURAL EQUATION MODELLING OF THE POPULATION DYNAMICAL EFFECTS OF CLIMATE

### The substantive ecological hypotheses

We assessed the structural and causal effects of large-scale climate, regional weather, population density and stochasticity on numeric recruitment and spatial dynamics of ducks using structural equations with latent constructs modelling (hereafter SEM; Bollen 1989; see Myers & Cadigan 1993 for a related ecological approach). As spatial and numeric recruitment processes were temporally and spatially uncoupled (Almaraz & Amat 2004), separate models will be constructed for both patterns. In our hypothetical models, we will assume brood recruitment ($\Delta N_b$) and spatial dynamics ($\Delta S_b$) to be affected by both rainfall ($W_{t-i}$, where $i$ stands for a time lag) and $\log_e$-population density [$X_{t-i} = \log_e(D_{t-i})$, see above], the later being affected as well by rainfall; that is, here we test the plausible hypothesis that rainfall can modulate population density (the number of birds per km$^2$ of wetland) by determining the number of available habitat patches (see Newton 1998 for examples with other waterfowl species), hence affecting brood recruitment in a non-additive way (*sensu* Stenseth *et al.* 2002). Additionally, if population density affects spatial dynamics, this would suggest that territoriality may exert a positive effect on spatial expansion, a common process in territorial birds (see Newton 1998). Rainfall is in turn affected by both the NAO ($U_{t-i}$) and the ENSO ($Z_{t-i}$), which we consider to be teleconnected in our model. Finally, we can assume that population density is the output of an imperfect measurement process, with potential implications on parameter estimation (Bollen 1989). Therefore, we will model *real* population density as a *latent* (unobserved) variable in our SEM, and consider measured population density just as an *indicator* of the unobserved dynamic process (see Bollen 1989 for further details). That is, we superimposed a measurement model, incorporating information on the observation errors of the measurement process, upon the structural model described by the substantive hypothesis. For reasons of space, in Appendix S1 (see Supplementary Material) we describe the construction of the full SEM from the assumptions made by a simulated measurement process. Figure 2 shows a path diagram depicting the topological relationships between the ecological and climatic variables, as assumed by the substantive hypotheses.

### The mathematical model

Putting the substantive hypotheses in mathematical form is straightforward; under standard assumptions (see below), we can write the general hypotheses as:

$$\Delta N_b = \gamma + \eta_1 X_{t-i} + \eta_2 W_{t-i} + \varepsilon_t \quad (1.1)$$

$$\Delta S_b = \gamma + \eta_1 X_{t-i} + \eta_2 W_{t-i} + \varepsilon_t \quad (1.2)$$

$$X_{t-i} = \tau + \eta_3 W_{t-i} + \varepsilon_t \quad (2)$$

$$W_{t-i} = \mu + \xi_1 U_{t-i} + \xi_2 Z_{t-i} + \varepsilon_t \quad (3)$$

©2004 Blackwell Publishing Ltd/CNRS

$$\xi_3 = \mathrm{Cov}(U_{t-i}, Z_{t-i}) \quad (4)$$

$$x_t = X_t[d_n]^{-1} + \delta_{x,t} \quad (5)$$

Each of the variables $\varepsilon_t$ is a set of independent and identically distributed (IID) random variables following a normal distribution, (see Fig. 2). Parameters in eqns 1–4 denote, respectively, the strength of density dependence ($\eta_1$); the magnitude of the abiotic effect on brood recruitment ($\eta_2$); the strength of the rainfall effect on population density ($\eta_3$); the NAO ($\xi_1$) and ENSO ($\xi_2$) effects on rainfall and the strength of the teleconnection of both hemispheric fluctuations ($\xi_3$). Additionally, parameters $\gamma$, $\tau$, $\mu$ are intercepts, and need not be estimated (Bollen 1989). Equation 5, which represent the connection between the measurement model and the structural model is described in detail in Appendix S1. In summary, as there are five measured variables in the above model, up to this point we have constructed two *population* variance–covariance matrix ($\boldsymbol{\Sigma}$; Bollen 1989), one for numeric recruitment and the other for spatial dynamics. For instance, the matrix for the numeric recruitment component would thus be

$$\boldsymbol{\Sigma} = \begin{bmatrix} \mathrm{Var}(\Delta N_\mathrm{b}) & \mathrm{Cov}(\Delta N_\mathrm{b}, X_t) & \mathrm{Cov}(\Delta N_\mathrm{b}, W_{t-i}) & \mathrm{Cov}(\Delta N_\mathrm{b}, U_{t-i}) & \mathrm{Cov}(\Delta N_\mathrm{b}, Z_{t-i}) \\ & \mathrm{Var}(X_t) & \mathrm{Cov}(X_t, W_{t-i}) & \mathrm{Cov}(X_t, U_{t-i}) & \mathrm{Cov}(X_t, Z_{t-i}) \\ & & \mathrm{Var}(W_{t-i}) & \mathrm{Cov}(W_{\mathrm{t}-1}, \mathrm{U}_{t-i}) & \mathrm{Cov}(W_{\mathrm{t}-1}, Z_{t-i}) \\ & & & \mathrm{Var}(U_{t-i}) & \mathrm{Cov}(U_{\mathrm{t}-1}, Z_{t-i}) \\ & & & & \mathrm{Var}(Z_{t-i}) \end{bmatrix}. \quad (6)$$

(ii) the interannual stochastic variability impacting on each endogenous variable ($\varepsilon_t$) is assumed to describe a white noise process with 0 mean and constant variance $\psi_i$; that is, $\varepsilon_t \sim N(0, \psi_{1-3})$ (iii) $\delta_{x,t} \sim N(0, \theta_x)$, where $\theta_x$ is the estimation error variance of population density (see Appendix S1); and (iv) NAO and ENSO proxy indexes were drawn from time-invariant, normal distributions with mean $v_i$ and constant variance $\zeta_i$; that is, $U_{t-1} \sim N(v_1, \zeta_1)$, $Z_{t-1} \sim N(v_2, \zeta_2)$. Collecting variances and covariances across terms, the *population* matrix $\boldsymbol{\Sigma}$ can now be rewritten as

$$\boldsymbol{\Sigma} = \begin{bmatrix} (\eta_1^2 + \eta_2^2)\varphi_1 + \psi_1 + \theta_\mathrm{x} & \eta_1\varphi_1 & \eta_2\varphi_2 & 0 & 0 \\ & (\eta_3^2)\varphi_1 + \psi_2 + \theta_\mathrm{x} & \eta_3\varphi_1 & 0 & 0 \\ & & (\xi_1^2 + \xi_2^2)\varphi_2 + \psi_3 & (\varphi_3 + \psi_3)\xi_1 & (\varphi_3 + \psi_3)\xi_2 \\ & & & \varsigma_1 & \xi_3 \\ & & & & \varsigma_2 \end{bmatrix}. \quad (7)$$

Figure 2 depicts the topological position of each covariance written in matrix 7.

At this step we used the data to test the hypothesis

$$\boldsymbol{\Sigma} = \boldsymbol{\Sigma}(\boldsymbol{\theta}) \quad (8)$$

where $\boldsymbol{\theta}$ is the vector containing the model parameters, and $\boldsymbol{\Sigma}(\boldsymbol{\theta})$ is the covariance matrix written as a function of the elements in $\boldsymbol{\theta}$ (Bollen 1989). The theoretical population matrix can be derived using linear covariance algebra and conditional probability theory. Sampling parameter estimates (i.e., sampling estimators of the population parameters in $\boldsymbol{\theta}$) were obtained by minimizing the discrepancy between the sampling variance–covariance matrix (**S**) and the expected (*population*) matrix given the causal structure and the data, using a generalized least squares (GLS) loss function (Bollen 1989; see Almaraz & Amat 2004). Monte Carlo simulation suggests that the statistical power of GLS covariance structures is greater than maximum-likelihood models in noisy data sets derived from short time series (P. Almaraz, unpublished data). Overall, from the parameter

## The statistical hypothesis

In order to estimate the biological parameters in eqns 1–5, a set of distributional assumptions regarding the model must be made (Bollen 1989; Myers & Cadigan 1993): (i) both log-transformed population density ($X_{t-i}$), and rainfall ($W_{t-i}$) were assumed to be drawn from time-invariant, normal distributions with means $\mu_i$ and constant variances $\varphi_i$; that is, $X_t \sim N(\mu_1, \varphi_1)$ and $W_t \sim N(\mu_2, \varphi_2)$;

©2004 Blackwell Publishing Ltd/CNRS

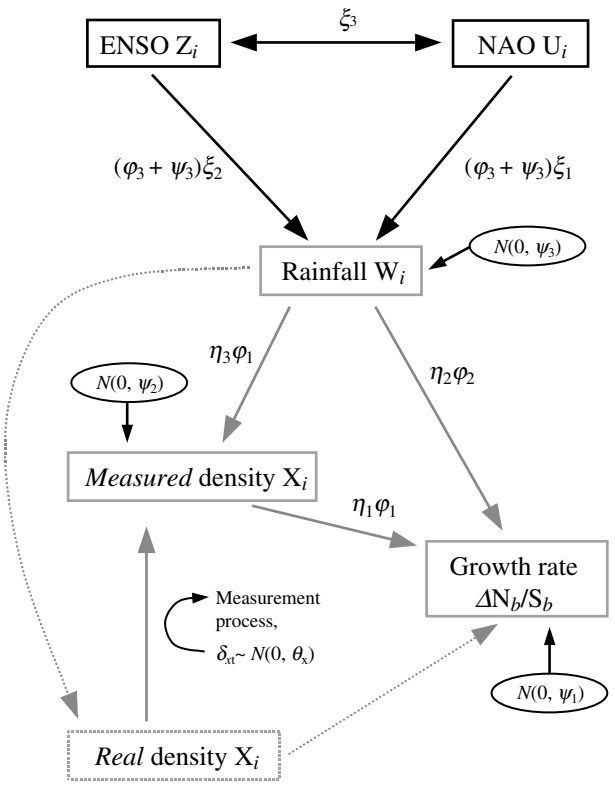


**Figure 2** Diagram of the full structural equation model depicting the large-scale climatic effects on *O. leucocephala* spatio-temporal dynamics through regional weather variability. The modelled spatial downscaling follows logically from the upper part of the graph to the lower part. Each box in the graph depicts a variable (modelled indicator if solid, unobserved latent if dotted) and each arrow depicts a causal relationship (if single-headed) or a simultaneous covariance (if double-headed) between the set of indicators (if solid) and constructs (if dotted). The ovals stand for the structural perturbation term of each endogenous variable. See the main text and Appendix S1 in the Supplementary Material for parameters and further descriptions.

values satisfying the condition imposed by eqn 8 we derived the goodness-of-fit of **S** to **Σ**, which is the central hypothesis of the present paper; specifically, statistical theory predicts that if **S** follows a Wishart distribution (a less restrictive statistical assumption than the multivariate normal) and the model is identified (the number of free parameters to be estimated from the model is smaller than the total variances and covariances of the variance–covariance matrix), the difference between **S** and **Σ** will asymptotically follow a chi-square distribution (Bollen 1989). Although our models are over-identified (see matrix 7 and Fig. 2), the exact sampling distribution of the goodness-of-fit statistic is seldom known (Bollen 1989). Therefore, uncertainty of point parameter and goodness-of-fit estimates of each variance–covariance structure was assessed with the bias-corrected bootstrap method (Efron & Tibshirani 1993). Because bootstrapped estimates do not assume any particular sampling distribution, this allowed us to relax the strong distributional assumptions made in matrix 7. One thousand bootstrapped covariance structures were used, and a range of 90% around the point estimate was considered given the severity of this method when working with small and biased samples (Efron & Tibshirani 1993).

The dimension of the model derived from matrix 7 can be reduced by considering the effects of large-scale climate as negligible, that is, by setting free parameters $\xi_1$ or $\xi_2$ to 0; additionally, by setting parameter $\eta_3$ to 0, models with just additive climatic effects can be tested against models with both additive and non-additive effects. Overall, six structural models (one *saturated* plus five *nested*; Bollen 1989) were estimated and tested for each component of the dynamics. In order to optimize the trade-off between the bias introduced in model estimation when relevant parameters are omitted and the overall variance inflation caused by an overparameterized model, information-theoretic [Akaike information criterion (AIC)] and approximate fit indexes [Brown-Cudeck cross-validation index (CVI)] were calculated for each of the covariance structures (Bollen 1989). Small AIC and CVI values suggest a high parsimony and a good fit of the model, respectively. Programming and analyses were conducted in the SEPATH module of STATISTICA 6.1 (StatSoft, Inc. 2003).

## RESULTS

### Testing the general substantive hypothesis

Results of the goodness-of-fit tests performed with the spatial and numeric SEMs are given in Table 1. Interestingly, *P*-values are large for nearly all of them, suggesting that the empirical covariance structures tested conforms to highly plausible hypotheses given the available data; moreover, the bootstrap estimated uncertainty of the chi-squared statistics yield very high confidence in the robustness of the results against violations of the distributional assumptions (the so-called Wishart distribution). The joint interpretation of the parsimony and approximate fit indexes, and the tests for multivariate normality suggest that the saturated model for numeric recruitment ($\Delta N_b[\xi_{1-3} + \eta_{1-3}]$) and the nested model with just NAO forcing and additive climatic effect for spatial dynamics ($\Delta S_b[\xi_1 + \eta_1 + \eta_2]$) are the best candidates given our initial hypotheses. Note, however, that the model $\Delta N_b[\xi_1 + \eta_{1-3}]$ is a slightly better model relative to the saturated one according to the above indices; nevertheless, the significant covariance between the NAO and the ENSO during the study period (see below) suggested that the saturated model should be selected instead. Additionally, the differences in AIC and

©2004 Blackwell Publishing Ltd/CNRS

**Table 1** Results of the goodness-of-fit tests for the structural models constructed

| Model | $\chi^2_{\text{d.f.}}$ | 90% BCCI | *P*-value | AIC | CVI | M-B Kappa |
|---|---|---|---|---|---|---|
| $\mathbf{\Delta N_b[\xi_{1-3} + \eta_{1-3}]}$ | $3.049_4$ | (0.178, 5.283) | 0.550 | 1.318 | 1.729 | −0.054 |
| $\Delta N_b[\xi_1 + \eta_{1-3}]$ | $0.148_2$ | (0.001, 2.104) | 0.929 | 0.850 | 1.170 | 0.018 |
| $\Delta N_b[\xi_2 + \eta_{1-3}]$ | $3.014_2$ | (1.072, 6.686) | 0.222 | 1.001 | 1.151 | −0.044 |
| $\Delta N_b[\xi_{1-3} + \eta_1 + \eta_2]$ | $5.137_5$ | (0.406, 6.739) | 0.399 | 1.323 | 1.809 | −0.054 |
| $\Delta N_b[\xi_1 + \eta_1 + \eta_2]$ | $2.819_3$ | (0.117, 4.524) | 0.420 | 0.885 | 1.148 | 0.018 |
| $\Delta N_b[\xi_2 + \eta_1 + \eta_2]$ | $5.102_3$ | (1.119, 7.352) | 0.164 | 1.005 | 1.269 | −0.044 |
| $\Delta S_b[\xi_{1-3} + \eta_{1-3}]$ | $0.671_4$ | (0.015, 2.867) | 0.955 | 1.193 | 1.728 | −0.150 |
| $\Delta S_b[\xi_1 + \eta_{1-3}]$ | $0.517_2$ | (0.006, 2.677) | 0.772 | 0.869 | 1.170 | −0.075 |
| $\Delta S_b[\xi_2 + \eta_{1-3}]$ | $0.152_2$ | (0.001, 1.720) | 0.927 | 0.850 | 1.151 | −0.203 |
| $\Delta S_b[\xi_{1-3} + \eta_1 + \eta_2]$ | $0.935_5$ | (0.194, 5.314) | 0.968 | 1.102 | 1.588 | −0.150 |
| $\mathbf{\Delta S_b[\xi_1 + \eta_1 + \eta_2]}$ | $0.784_3$ | (0.015, 1.950) | 0.853 | 0.778 | 1.041 | −0.075 |
| $\Delta S_b[\xi_2 + \eta_1 + \eta_2]$ | $0.436_3$ | (0.003, 1.519) | 0.933 | 0.760 | 1.023 | −0.203 |

Each model is denoted by the dynamic component modelled (numeric, $\Delta N_b$, or spatial, $\Delta S_b$) and the parameters specifically affecting it, represented within square brackets (see main text for descriptions). The point estimate of the chi-squared statistic, the 90% bias-corrected bootstrap confidence interval of the estimate (BCCI), and the associated *P*-value of the goodness-of-fit test are shown. In addition, the Akaike Information Criterion (AIC), the Browne-Cudeck Cross-Validation Index (CVI), and the Mardia-based (M-B) Kappa, which test for the sphericity of the covariance matrix are also given. M-B Kappa values close to 0 suggest that the covariance matrix do not depart significantly from a multivariate normal matrix (Bollen 1989). The best model for each dynamic component is given in bold.

CVI among the models tested were negligible, so non-additive climatic effects on spatial dynamics through population density cannot be excluded (compare $\Delta S_b[\xi_1 + \eta_1 + \eta_2]$ against $\Delta S_b[\xi_{1-3} + \eta_{1-3}]$ in Table 1).

## Testing individual covariances within the central hypothesis

Table 2 shows the univariate standardize partial regression coefficients derived from the covariances in matrix 7 for the best structural models selected above; however, we show parameter values for the model $\Delta S_b[\xi_1 + \eta_{1-3}]$ instead of the 'best' model in order to compare the behaviour of the SEM when simulated estimation error variance is taken into account (see Appendix S1). Results suggest differential roles for climatic variability and population density during numeric recruitment and range dynamics. In this sense, population density had a larger effect on numeric recruitment ($\eta_1 = -0.433$) than did climatic variability ($\eta_2 = 0.386$), the opposite applying for range dynamics. Bootstrap estimated uncertainty of point parameter values were generally larger than normality-based values across all models (Table 2), with notable discrepancies in some cases; additionally, both the magnitude of density dependence and the strength of the climatic effect on population density slightly decreased when simulated estimation error variance

**Table 2** Parameter estimates for models $\Delta N_b[\xi_{1-3} + \eta_{1-3}]$ and $\Delta S_b[\xi_1 + \eta_{1-3}]$ in Table 1

| Model, parameters and paths | Estimate | 90% NT CI | 90% BCCI |
|---|---|---|---|
| $\mathbf{\Delta N_b[\xi_{1-3} + \eta_{1-3}]}$ | | | |
| $\eta_1$ (Density → recruitment) | −0.433 | (−0.746, −0.119) | (−0.717, 0.015) |
| $\eta_2$ (Rain → recruitment) | 0.386 | (0.061, 0.712) | (−0.250, 0.811) |
| $\eta_3$ (Rain → density) | −0.434 | (−0.761, −0.107) | (−0.665, 0.273) |
| $\xi_1$ (NAO → rain) | −0.155 | (−0.451, 0.141) | (−0.590, 0.240) |
| $\xi_2$ (ENSO → rain) | 0.667 | (0.407, 0.926) | (0.244, 0.851) |
| $\xi_3$ (ENSO↔NAO) | −0.462 | (−0.774, −0.150) | (−0.693, 0.085) |
| $\mathbf{\Delta S_b[\xi_1 + \eta_{1-3}]}$ | | | |
| $\eta_1$ (Density → expansion) | 0.357 | (0.036, 0.678) | (−0.450, 0.716) |
| $\eta_2$ (Rain → expansion) | 0.370 | (0.055, 0.685) | (−0.061, 0.569) |
| $\eta_3$ (Rain → density) | −0.127 | (−0.507, 0.254) | (−0.431, 0.295) |
| $\xi_1$ (NAO → rain) | −0.592 | (−0.843, −0.341) | (−0.661, −0.215) |

Path arrows within each model denote hypothesized teleconnections (↔) and directed explicit exogenous sources of variability (→). Shown are point estimates of parameters, along with their 90% confidence intervals estimated according to the normal theory (NT CI) and from a set of 1000 bootstrapped samples using the bias-corrected method (BCCI).

©2004 Blackwell Publishing Ltd/CNRS

was taken into account, although the overall effects of sampling variability on the goodness-of-fit was negligible (see Appendix S1). Keeping this in mind, the best model for numeric recruitment yielded robust coefficients for both the boreal summer NAO–ENSO teleconnection and the ENSO link with rainfall variability (Table 2). Notably, when included together with the ENSO in the saturated model, the NAO effect on regional weather seems to be cancelled out. A weak coefficient is also found for the 1-year lagged rainfall effect on population density. On the other hand, the best model for the spatial dynamics subset exclude both the ENSO forcing and non-additive climate effects, while suggesting that the wintering phase of the NAO exerts an indirect negative effect on range dynamics through regional meteorological conditions (Table 2).

### Comparison of SEM to standard ecological time-series modelling approaches

In order to compare the SEM method to traditional ecological time-series modelling approaches, we constructed two autoregressive-type models with environmental covariates (e.g. Aanes *et al.* 2002; Lima *et al.* 2002; Lekve *et al.* 2003) using the same variables depicted in Fig. 2 (i.e. we deleted any topological complexity from the model without reducing its dimensionality). In brief, the models would have the form

$$\Delta N_b = a + bX_t + cW_{t-i} + dU_{t-i} + eZ_{t-i} + \sigma\varepsilon_t \qquad (9.1)$$

$$\Delta S_b = a + bX_t + cW_{t-i} + dU_{t-i} + eZ_{t-i} + \sigma\varepsilon_t \qquad (9.2)$$

**Table 3** Summary of the general linear modelling (GLM) of the extrinsic (ENSO, NAO and regional rainfall) and intrinsic (population density) effects on the numeric and spatial dynamics of *O. leucocephala* in Spain, 1980–2000

| Predictor | Estimate | SE | *t*-test | *P*-value |
|---|---|---|---|---|
| Numeric recruitment ($\Delta N_b$) | | | | |
| ENSO | −0.351 | 0.247 | −1.421 | 0.176 |
| NAO | −0.031 | 0.199 | −0.156 | 0.877 |
| Rainfall | 0.534 | 0.270 | 1.980 | 0.067 |
| Population density | −0.463 | 0.196 | −2.363 | 0.032 |
| Spatial dynamics ($\Delta S_b$) | | | | |
| ENSO | 0.062 | 0.224 | 0.277 | 0.786 |
| NAO | 0.061 | 0.278 | 0.220 | 0.828 |
| Rainfall | 0.406 | 0.275 | 1.476 | 0.161 |
| Population density | 0.373 | 0.229 | 1.633 | 0.123 |

The GLM (normal error structure and identity link function) was derived from a standard autoregressive model with environmental effects included, besides population density (see text). Shown are point parameter estimates and associated standard errors (SE), and the value of the Student's *t*-test for each estimate.

Table 3 summarizes the results from the fitting of such models using a general linear model (GLM). The overall fitting of the GLM to the numeric subset was good ($R^2 = 0.44$; likelihood-ratio test: $\chi^2_4 = 16.25$, $P = 0.003$), but point parameter estimates included large uncertainties except for density ($P = 0.032$) and rainfall ($P = 0.067$). On the other hand, the fitting of the GLM to the spatial subset was poor ($R^2 = 0.05$, $\chi^2_4 = 5.75$, $P = 0.219$), with non-significant parameter estimates ($P > 0.10$ in all cases; Table 3). Therefore, in contrast to standard approaches, SEM results suggest a rather complex web of 'cascading effects' of climate in the dynamics of *O. leucocephala,* including non-additive effects for the numeric dynamics; moreover, these effects seem to differ markedly between the spatial and numeric components of the dynamics, with a complex causal structure in the numeric recruitment subset (fully captured by the saturated model shown in Fig. 2) and a rather less complex structure in the spatial subset.

## DISCUSSION

The effects of recent climate change are usually exerted through changes in precipitation and temperature patterns (Mooney *et al.* 2001; Stenseth *et al.* 2002; Root *et al.* 2003). Precipitations in the south-western Palaearctic decreased at a rate of 20% per decade during the last 30 years (Mooney *et al.* 2001), which is among the largest rates observed throughout the planet (IPCC 2001). Although some ecological responses to climate warming have been recently identified across this area, they are concerned with either phenological shifts (Peñuelas *et al.* 2002) or changes in breeding parameters (Sanz *et al.* 2003) correlated with linear trends in temperature. Hence, to our knowledge this is the first time that the two major planetary sources of interannual climatic variability are consistently linked to an ecological process in this region. Moreover, our study is the first to include explicitly and simultaneously connections between regional weather conditions and hemispheric climatic fluctuations in a single model describing the dynamics of a natural population. As shown, these complex relationships would not have been uncovered with traditional modelling techniques, so the structural approach adopted in this study provides our results with strong inferential power (Bollen 1989).

Interestingly enough, our previous findings (Almaraz & Amat 2004) suggested that the spatial and numeric dynamic abundance patterns were temporally uncoupled, so different mechanisms should be involved in the processes generating the patterns observed. The present paper is revealing in this sense; for instance, increased rainfall during low NAO winters prompted the spatial expansion of the population from breeding to wintering, probably by increasing the number of available wetlands after the dry Mediterranean

©2004 Blackwell Publishing Ltd/CNRS

summer; on the other hand, as proposed in our substantive hypothesis, the 1-year lagged rainfall signal on population density during numeric recruitment suggest that a low ENSO index during austral winters cause a range contraction through a reduction in western Mediterranean summer rainfall: because range size correlates strongly with range surface and with population size, an increase in population density is thus expected after dry years. For example, the strong El Niño events of 1982–83, 1986–87 and 1997–98 (Trenberth *et al.* 1998; IPCC 2001) were linked to high summer rainfall values in the study area during the same years, and with extremely low breeding densities the year after; accordingly, large recruitment episodes coupled with these low densities were evident in the population (Fig. 3). Therefore, here we have provided empirical evidence that regional meteorological conditions correlated with hemispheric fluctuations in climate are independently affecting the spatial and numeric dynamics of ducks in a non-additive way (Stenseth *et al.* 2002) by indirectly modulating the strength of density dependence impacting on the population. Previous evidence also suggested non-additive effects of climate in a Dipper *Cinclus cinclus* population in Norway (Sæther *et al.* 2000) and in the Soay Sheep population of Hirta Island, off Scotland (Coulson *et al.* 2001). However, while these studies model interactive effects of climate as a direct impact on the density-dependent parameter (see Stenseth *et al.* 2002), here we have shown that climate directly modulates population density in *O. leucocephala,* which is indeed a function of habitat availability (see also Newton 1998); population density, when measured on a spatially implicit basis, would thus be an environment-dependent state variable. Hence, our study suggests a novel pathway for non-additive effects of climate, which may be

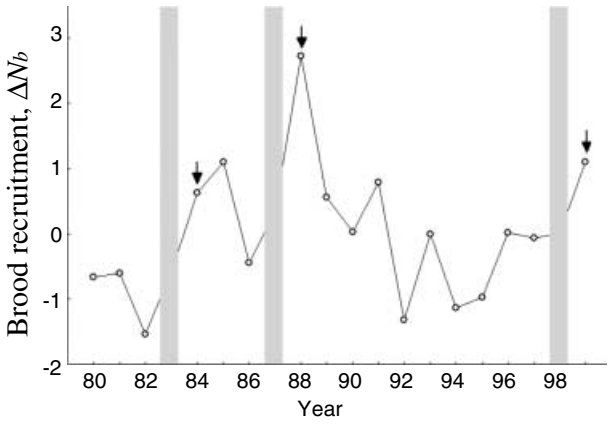


**Figure 3** Standardized brood recruitment dynamics of *O. leucocephala* in Spain during the period 1980–2000. Vertical grey bars in the graph denote strong El Niño years, according to the IPCC (2001), while arrows indicate the 1-year lagged recruitment events apparent after each El Niño episode.

important in species with patchy populations inhabiting temporary wetlands (see e.g. Harrison 1994).

Given ongoing global climate change (IPCC 2001), a great deal of research is being devoted to the exploration of climatic interactions between tropical and extratropical regions (e.g. Rodó *et al.* 1997; Moron & Ward 1998; Trenberth *et al.* 1998; van Oldenborgh *et al.* 2000; Hoerling *et al.* 2001; Rodó 2001; Mélice & Servain 2003; Rodó 2003). Signals of the ENSO on extratropical rainfall variability have been found, for instance, on the Iberian Peninsula (Rodó *et al.* 1997), Central Europe (van Oldenborgh *et al.* 2000), and the Middle East (Yakir *et al.* 1996). Nevertheless, the amount of global rainfall variability correlated with the ENSO is uncertain (Allan *et al.* 1996; Dai *et al.* 1997) and no clear consensus exists among authors (IPCC 2001). This uncertainty complicates the exploration of possible inter-hemispheric teleconnections between ocean/atmosphere couplings taking place in the eastern equatorial Pacific and ecological processes of the Northern Hemisphere (Rodó 2003). In this sense, the Mediterranean basin is forecasted by several global circulation models (GCMs) as one of the most affected by future climate change under scenarios of doubled concentrations of greenhouse gases (IPCC 2001), with a 5–15% of reduction in rainfall relative to current levels by the year 2100 (IPCC 2001; Mooney *et al.* 2001). In addition, high resolution GCMs predict more frequent El Niño events in similar scenarios (Timmermann *et al.* 1999; IPCC 2001), and also a future persistence of the ongoing positive NAO phase (Visbeck *et al.* 2001). Notably, a remarkable result of our study was the positive linkage detected between the summer ENSO index and regional rainfall in the south-western Mediterranean, an unexpected coupling according to recent evidence (Rodó *et al.* 1997; Rodó & Comín 2000). Moreover, a significant teleconnection was found between the NAO and the ENSO during boreal summer throughout the study period. Although no clear connection was previously suggested for the North Atlantic grid and the Pacific equatorial basin (Rodó *et al.* 1997; but see Hoerling *et al.* 2001), a further analysis shows that the strength of this boreal summer covariation has been increasing during the last 40 years (Fig. 1b). Thus, as standard GCMs forecast a counterintuitive dramatic decrease in summer rainfall for this region in the following years, any prediction on the effects of future climate change on ecological processes in the south-western Palaearctic might be largely precluded by these results. However, they suggest that ecologically similar species might be responding in a same way to large-scale climatic fluctuations in this geographical area, and stress the need for further research on this topic.

In conclusion, our results add to some recent findings (Sæther *et al.* 2000; Bjørnstad & Grenfell 2001; Coulson *et al.* 2001; Thompson & Ollason 2001; Rodó *et al.* 2003; Durant

©2004 Blackwell Publishing Ltd/CNRS

*et al.* 2004) to suggest a complex intertwining between endogenous (e.g. density dependence), exogenous (climatic variability) and stochastic forces in population dynamics, and extend them by suggesting that future research on population regulation might gain insight by focusing on how these forces are structurally interrelated to generate a dynamical pattern at the population level. For instance, our data have shown that whereas climatic teleconnections can take place within a few weeks, these couplings can generate biological signals with several time lags, and with complex non-additive effects on both the spatial and numeric components of the dynamics. Moreover, as a further challenge to ecological research under climate warming scenarios, they suggest that the effects of large-scale climatic anomalies on population dynamics can be very strong even in geographical areas exceptionally distant from their centres of action. New ecological time-series modelling techniques, such as the structural modelling with latent constructs approach, will be instrumental in untangling complex interactions in the climate–ecology interface.

## ACKNOWLEDGEMENTS

Comments from Jordi Bascompte, José M. Gómez, Andy J. Green, Mauricio Lima and Nils Chr. Stenseth on previous versions of this manuscript were very valuable. During manuscript preparation we were supported by funds from Plan Andaluz de Investigación (research group RNM 0105), and P. A. was supported by a Spanish Ornithological Society/ BirdLife International Novel Researchers grant, 2002.

## SUPPLEMENTARY MATERIAL

The following material is available from http://www.blackwellpublishing.com/products/journals/suppmat/ELE/ELE612/ELE612sm.htm

**Appendix S1** Measurement error and estimation error variance.

## REFERENCES

Aanes, R., Sæther, B.-E., Smith, F.M., Cooper, E.J., Wookey, P.A. & Øritsland, N.A. (2002). The Arctic oscillation predicts effects of climate change in two trophic levels in a high-arctic ecosystem. *Ecol. Lett.*, 5, 445–453.

Allan, R., Lindeasy, J. & Parker, D. (1996). *El Niño Southern Oscillation and Climate Variability*. CSIRO, Collinwood.

Almaraz, P. & Amat, J.A. (2004). Multi-annual spatial and numeric dynamics of the White-headed duck (*Oxyura leucocephala*) in southern Europe: seasonality, density dependence and climatic variability. *J. Anim. Ecol.*, in press.

Bjørnstad, O.N. & Grenfell, B.T. (2001). Noisy clockwork: time series analysis of population fluctuations in animals. *Science*, 293, 638–643.

Bollen, K.A. (1989). *Structural Equations with Latent Variables*. John Wiley and Sons, New York.

Chávez, F.P., Ryan, J., Lluch-Cota, S.E. & Ñiquez, M. (2003). From anchovies to sardines and back: multidecadal change in the Pacific Ocean. *Science*, 299, 217–221.

Christensen, J.H. & Christensen, O.B. (2003). Severe summertime flooding in Europe. *Nature*, 421, 805–806.

Coulson, T., Catchpole, E.A., Albon, S.D., Morgan, B.J.T., Pemberton, J.M., Clutton-Brock, T. H. *et al.* (2001). Age, sex, density, winter weather, and population crashes in Shoay sheep. *Science*, 295, 1528–1531.

Dai, A., Fung, I.Y. & Del Genio, A.D. (1997). Surface observed global land precipitation variations during 1900–88. *J. Clim.*, 10, 2943–2962.

Durant, J.M., Anker-Nilseen, T., Hjermann, D.Ø. & Stenseth, N.C. (2004). Regime shifts in the breeding of an Atlantic puffin population. *Ecol. Lett.*, 7, 388–394.

Efron, B. & Tibshirani, R. (1993). *An Introduction to the Bootstrap*. Chapman & Hall, New York.

Green, A.J. & Hughes, B. (2001). White-headed duck (*Oxyura leucocephala*). In: *BWP Update: The Journal of the Birds of the Western Palaearctic*, Vol. 3 (ed. Parkin, D.B.). Oxford University Press, Oxford, pp. 79–90.

Harrison, S. (1994). Metapopulations and conservation. In: *Large-scale ecology and conservation biology* (eds Edwards, P.J., May, R.M. & Webb, N.R.). Blackwell Scientific, Oxford, pp. 111–128.

Hoerling, M.P., Hurrell, J.W. & Xu, T. (2001). Tropical origins for recent North Atlantic climate change. *Science*, 292, 90–92.

Holmgren, M., Scheffer, M., Ezcurra, E., Gutiérrez, J.R. & Mohren, G.M.J. (2001). El Niño effects on the dynamics of terrestrial ecosystems. *Trends Ecol. Evol.*, 16, 89–94.

Hurrell, J.W. (1995). Decadal trends in the North Atlantic Oscillation: regional temperatures and precipitation. *Science*, 269, 676–679.

IPCC (2001). *Climate Change 2001: Third Assessment Report of the Intergovernmental Panel on Climate Change WG I & II*. Cambridge University Press, Cambridge.

Lekve, K., Stenseth, N.C., Johansen, R., Lingjærde, O.C., Gjøsæter, J. (2003). Richness dependence and climatic forcing as regulating processes of coastal fish-species richness. *Ecol. Lett.*, 6, 428–439.

Lima, M., Stenseth, N.C. & Jaksic, F. (2002). Food web structure and climate effects on the dynamics of small mammals and owls in semi-arid Chile. *Ecol. Lett.*, 5, 273–284.

Mélice, J.-L. & Servain, J. (2003). The tropical Atlantic meridional SST gradient index and its relationships with the SOI, NAO and Southern Ocean. *Clim. Dyn.*, 20, 447–464.

Mooney, H.A., Arroyo, M.T.K., Bond, W.J., Canadell, J., Hobbs, R.J., Lavorel, S. *et al.* (2001). Mediterranean ecosystems. In: *Global Biodiversity in a Changing Environment. Scenarios for the 21st Century* (eds Chapin, F.S., Sala, O.E. & Huber-Sannwald, E.). Springer-Verlag, New York, pp. 157–199.

Moron, V. & Ward, M.N. (1998). ENSO teleconnections with climate variability in the European and African sectors. *Weather*, 53, 287–295.

Myers, R.A. & Cadigan, N.G. (1993). Density-dependent juvenile mortality in marine demersal fish. *Can. J. Fish. Aquat. Sci.*, 50, 1576–1590.

Newton, I. (1998). *Population Limitation in Birds*. Academic Press, San Diego.

©2004 Blackwell Publishing Ltd/CNRS

Ogutu, J.O. & Owen-Smith, N. (2003). ENSO, rainfall and temperature influences on extreme population declines among African savanna ungulates. *Ecol. Lett.*, 6, 412–419.

van Oldenborgh, G., Burgers, G. & Tank, A.K. (2000). On the El Niño teleconnection to spring precipitation in Europe. *Int. J. Climatol.*, 20, 565–574.

Ottersen, G., Planque, B., Belgrano, A., Post, E., Reid, P.C. & Stenseth, N.C. (2001). Ecological effects of the North Atlantic Oscillation. *Oecologia*, 128, 1–14.

Peñuelas, J., Filella, I. & Comas, P. (2002). Changed plant and animal life cycles from 1950 to 2000 in the Mediterranean region. *Glob. Chan. Biol.*, 8, 531–544.

Plisnier, P.D., Serneels, S. & Lambin, E.F. (2000). Impact of ENSO on East African ecosystems: a multivariate analysis based on climate and remote sensing data. *Global Ecol. Biog.*, 9, 418–497.

Polis, G.A., Hurd, S.D., Jackson, C.T. & Sánchez-Piñero, F. (1997). El Niño effects on the dynamics and control of an island ecosystem in the Gulf of California. *Ecology*, 78, 1884–1897.

Ramos, J.A., Maul, A.M., Ayrton, V., Bullock, I., Hunter, J., Bowler, J. *et al.* (2002). Influence of local and large-scale weather events and timing of breeding on tropical roseate tern reproductive parameters. *Mar. Ecol. Prog. Ser.*, 243, 271–279.

Rodó, X. (2001). Reversal of three global atmospheric fields linking changes in SST anomalies in the Pacific, Atlantic and Indian oceans at tropical latitudes and midlatitudes. *Clim. Dyn.*, 18, 203–217.

Rodó, X. (2003). Interactions between the tropics and extratropics. In: *Global Climate: Current Research and Uncertainties in the Climate System* (eds Rodó, X. & Comín, F.A.). Springer-Verlag, Berlin, pp. 237–274.

Rodó, X. & Comín, F.A. (2000). Links between large-scale anomalies, rainfall and wine quality in the Iberian Peninsula during the last three decades. *Glob. Chan. Biol.*, 6, 267–273.

Rodó, X., Baert, E. & Comín, F.A. (1997). Variations in seasonal rainfall in Southern Europe during the present century: relationships with the North Atlantic Oscillation and the El Niño-Southern Oscillation. *Clim. Dyn.*, 13, 275–284.

Rodó, X., Pascual, M., Fuchs, G., Faruque, A.S.G. (2003) ENSO and cholera: a nonstationary link related to climate change? *Proc. Natl Acad. Sci. USA*, 99, 12901–12906.

Root, T.L., Price, J.T., Hall, K.R., Schneider, S.H., Rosenzweig, C. & Pounds, J.A. (2003). Fingerprints of global warming on wild animals and plants. *Nature*, 421, 57–60.

Sæther, B.-E., Tufto, J., Engen, S., Jerstad, K., Røstad, O .W. *et al.* (2000). Population dynamical consequences of climate change for a small temperate songbird. *Science*, 287, 854–856.

Sanz, J.J., Potti, J., Moreno, J., Merino, S. & Frías, O. (2003). Climate change and fitness components of a migratory bird breeding in the Mediterranean region. *Glob. Chan. Biol.*, 9, 1–12.

Sillet, T.C., Holmes, R.T. & Sherry, T.W. (2000). Impacts of a global climate cycle on population dynamics of a migratory songbird. *Science*, 288, 2040–2042.

StatSoft, Inc. (2003). *STATISTICA (Data Analysis Software System)*, version 6. StatSoft, Inc., Tulsa, OK.

Stenseth, N.C., Mysterud, A., Ottersen, G., Hurrell, J.W., Chan, K.-S. & Lima, M. (2002). Ecological effects of climate fluctuations. *Science*, 297, 1292–1296.

Stenseth, N.C., Ottersen, G., Hurrell, J.W., Mysterud, A., Lima, M., Chan, K.-S. *et al.* (2003). Studying climate effects on ecology through the use of climate indices: the North Atlantic Oscillation, El Niño Southern Oscillation and beyond. *Proc. R. Soc. Lond. B*, 270, 2087–2096.

Thompson, P.M. & Ollason, J.C. (2001). Lagged effects of ocean climate change on fulmar population dynamics. *Nature*, 413, 417–420.

Timmermann, A., Oberhuber, J. Bacher, A., Esch, M., Latif, M. & Roeckner. E. (1999). Increased El Niño frequency in a climate model forced by future greenhouse warming. *Nature*, 398, 694–697.

Trenberth, K.E., Branstator, G.W., Karoly, D., Kumar, A., Lau, N.C. & Ropelewski, C. (1998). Progress during TOGA in understanding and modelling global teleconnections associated with tropical sea surface temperatures. *J. Geophys. Res.*, 103, 14291–14324.

Visbeck, M.H., Hurrel, J.W., Polvani, L & Cullen, H.M. (2001). The North Atlantic Oscillation: past, present, and future. *Proc. Natl Acad. Sci. USA*, 98, 12876–12877.

Wolter, K. & Timlin, M.S. (1993). Monitoring ENSO in COADS with a seasonally adjusted principal component index. In: *Proceedings of the 17th Climate Diagnostics Workshop* (NOAA/N MC/CAC, NSSL, Oklahoma Climate Survey, CIMMS and the School of Meteorology and University of Oklahoma). University of Oklahoma, Norman, pp. 52–57.

Yakir, D., Lev-Yadun, S. & Zangvil, A. (1996). El Niño and tree ring growth near Jerusalem over the last 20 years. *Glob. Chan. Biol.*, 2, 97–101.

Editor, M. Lambrechts
Manuscript received 29 February 2004
First decision made 30 March 2004
Manuscript accepted 16 April 2004

©2004 Blackwell Publishing Ltd/CNRS